Research Journal of Applied Sciences, Engineering and Technology 7(18): 3821-3836, 2014
DOI:10.19026/rjaset.7.739
ISSN: 2040-7459; e-ISSN: 2040-7467

Submitted: November 04, 2013 Accepted: November 13, 2013 Published: May 10, 2014

Research Article

Research on Fault Diagnosis System of a Diesel Engine Based on Wavelet Analysis and LabVIEW Software

[1,2]Eidam Ahmed Hebiel, [1]Zhu Zhou, [1]Dong Sheng Wang, [1]Liu Jie, [1]Mohamed Ahmed Elbashier, [1]Wen Dongdong, [1]Li Peng and [1]Li Xiaoyu
[1]Department of Agricultural Engineering Automation and Measurement Technology Research Section, College of Engineering, Huazhong Agricultural University, Wuhan, China
[2]Department of Agricultural Engineering, Faculty of Natural Resources and Environmental Studies, University of Western Kordofan, Elnahoud, Sudan

Abstract: Experiment presented in this study, used vibration data obtained from a four-stroke, 295 diesel engine. Fault of the internal-combustion engine was detected by using the vibration signals of the cylinder head. The fault diagnosis system was designed and constructed for inspecting the status and fault diagnosis of a diesel engine based on discrete wavelet analysis and LabVIEW software. The cylinder-head vibration signals were captured through a piezoelectric acceleration sensor, that was attached to a surface of the cylinder head of the engine, while the engine was running at two speeds (620 and 1300 rpm) and two loads (15 and 45 N·m). Data was gathered from five different conditions, associated with the cylinder head such as single cylinder shortage, double cylinders shortage, intake manifold obstruction, exhaust manifold obstruction and normal condition. After decomposing the vibration signals into some of the details and approximations coefficients with db5 mother wavelet and decomposition level 5, the energies were extracted from each frequency sub-band of healthy and unhealthy conditions as a feature of engine fault diagnosis. By doing so, normal and abnormal conditions behavior could be effectively distinguished by comparing the energy accumulations of each sub-band. The results showed that detection of fault by discrete wavelet analysis is practicable. Finally, two techniques, Back-Propagation Neural Network (BPNN) and Support Victor Machine (SVM) were applied to the signal that was collected from the diesel engine head. The experimental results showed that BPNN was more effective in fault diagnosis of the internal-combustion engine, with various fault conditions, than SVM.

Keywords: Diesel engine, fault detection, internal-combustion engine, LabVIEW, vibration signal, wavelet analysis

INTRODUCTION

Diesel engine is a main component in machinery and represents the heart of any vehicles. Therefore, it has gained great attention in the field of condition monitoring. For many decades, the only way of diagnosing and locating faults was by using biological senses. At that time, everything was based on observing, listening, smelling and touching different parts of the system. Later, a greater flow of accurate fault information was enabled by introducing measuring equipment and nowadays computers made possible of a dramatic progress in fault detection and identification. Fault detection in internal-combustion engines often requires the understanding of the dynamic and chemical processes that taking place inside an engine, which are difficult to model accurately (Chandroth and Staszewski, 1999). Most recently, diesel engines have expected to meet both fuel-economy requirements and pollutant emissions regulations, which are continuously becoming more rigorous. Good fuel and air mixture preparation is a key factor in meeting these requirements. Among the common internal-combustion engine faults, are the faults that affect the engine efficiency and may increase the emissions of unburned hydrocarbon, which caused by poor air to fuel ratios (Parlak *et al*., 2005) Diesel engine was used widely in many fields of applications. When the engine produced an abnormal vibration, it would not only make the vibration of the engine body itself increase, but also motivate the vibration inside machine parts and all kinds of accessories, as a result, it could cause a variety of shock and vibration damage. Features from vibration signals may be extracted in the time-domain (Ftoutou *et al*., 2011), frequency-domain (Carlucci *et al*., 2006) and time-frequency domain (Wang *et al*., 2008). The frequency-domain analysis is generally considered the most adequate signal-processing tool for the non-stationary diesel engine vibration. The method for developing analysis process is studied in this study in

Corresponding Author: Li Xiaoyu, Department of Agricultural Engineering Automation and Measurement Technology Research Section, College of Engineering, Huazhong Agricultural University, Wuhan, China

order to monitor four-stroke, 2 cylinders 295 diesel engine, using vibration signal. Vibration signal was acquired through piezoelectric acceleration sensors attached to a surface of the cylinder head of the engine using LabVIEW program. This signal was analyzed by using frequency-domain techniques to determine various parameters. Then the engine states could be predicted. Moreover, vibration signal detected on the diesel engine is composed of various events that associated with some mechanical processes in the engine. All events were combined to create a complicated vibration signal. This signal could be mapped onto various processes associated with a cylinder head such as one cylinder shortage, double cylinders shortage, intake manifold obstruction, exhaust manifold obstruction and normal condition, by using discrete wavelet transform method based on LabVIEW software. To achieve the above objectives, two sets of tests will be conducted:

- Setting up of the diesel engine to allow observations of the vibration signal characteristics when the diesel engine is running at a healthy condition.
- Setting up of the diesel engine in order to allow observations of the vibration signal characteristics when the diesel engine is suffering from abnormal conditions.

The signals will be analyzed by using the frequency-domain techniques. The results or information extracting from the analyzing of these signals related to engine processes can be used to identify or diagnosis faults by comparing detected deviations between normal and abnormal conditions in the engine (Girdhar *et al*., 2004).

MATERIALS AND HARDWARE DESIGN OF THE FAULT DETECTION

Diesel engine test of experimental study: The diesel engine used in this experiment was a 295 diesel engine. The engine has an excellent technical performance and operating stability. The specifications of the 295 diesel engine were shown in Table 1.

The diesel engine fault diagnosis system, Data Acquisition (DAQ) of monitoring and tools of signal collected, based on LabVIEW virtual instrument was shown in Fig. 1.

The dynamometer CW40, manufactured by Xiangjiang Power Testing Instrument Co. Ltd., was used in this experiment to measure and control the engine torque and speed. National Instrument PCI 6040 E card and LabVIEW software were used for data acquisition. Data was acquired in the card that placed directly inside the computer and used as an interface in order to control the plant in real time environment. Two Piezoelectric acceleration sensors-type CA-YD-106A were used; these sensors are small, highly sensitive and light in weight. Since the voltage signal from the sensor is very weak, the multi-Channel charge amplifier YE5853A was used to facilitate later observation, acquisition and signal analysis and processing. A SCB-68 shielded connection box with 68 screw terminals, for easy connection to the National Instruments 68-pin product, was used in this experiment. A Lenovo computer Pentium 4 with 3.00 GHz processor, 512 MB RAM and 80 GB HD was used. Feature extraction and data analysis were performed in a MATLAB 2010b program.

Table 1: Main design features of the test 295 diesel engine

Items	Parameters	Items	Parameters
Type	Vertical, four-stroke	Rated speed	1500 rpm
Number of cylinders	2	Dimensions	810×598×1514 mm
Bore×stroke	95×115 mm	Cooling system	Water cooling
Rated power	13.5 kW	weight	345 kg
Inlet	Naturally aspirated		

Fig. 1: Diesel engine fault diagnosis system, physical map

Fig. 2: The position of sensors on the diesel engine head

Sensors installation on the diesel engine head: Vibration signals have been measured using the most sensitive piezoelectric acceleration sensors, which were placed on the cylinders head bolts. The bolts tighten the cylinder head on the engine body and engine fundamental parts. These bolts have a direct impact on engine vibration. The position of the sensors on the internal-combustion diesel engine was shown in Fig. 2.

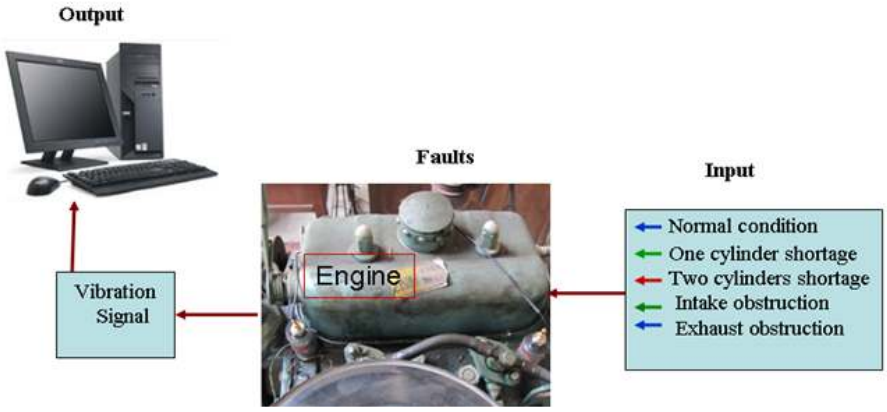

Fig. 3: On-line condition monitoring

Setting up of the experiment: The vibration data obtained from the tested diesel engine was used in this experiment. Data was gathered from five different conditions, which are associated with the cylinder head such as single cylinder shortage, double cylinders shortage, intake manifold obstruction, exhaust manifold obstruction and healthy condition. Single and double cylinders shortages were designed by artificially cutting diesel fuel route, while intake and exhaust manifolds obstruction were designed by placing a gasket in the opening between air inlet/exhaust outlet manifold pipe, respectively and engine body in order to decrease the normal opening of the air inlet and exhaust outlet. The engine speeds in this experiment were 620 and 1300 rpm; while the loads torque were 15 and 45 N·m. The On-line condition monitoring can be shown in Fig. 3.

The selection of sampling frequency and points: In the diesel engine, the frequency of the excited vibration was changed according to the alter of its source, speed and load. Some trials have shown that, the diesel engine's head vibration frequency will be about 10 kHz (Liu *et al*., 1999). For each of the above-mentioned five operating conditions, two speeds and two loads were used, then for each treatment; a signal was collected from the engine's head by using of the sensor. The signal was transferred into the computer through the data-acquisition units. One hundred and one amplitudes were randomly selected for each of the above mentioned treatments. The rate of the sample taken in this experiment was 20 kHz or 20 k samples per second as a floating-point data. The time duration of each vibration signal was 4 sec; and 5000 points were captured from each second. Since this rate of the sampling is too difficult to analyze; therefore, only 4096 samples were randomly chosen in order to facilitate the analysis process.

Vibration signal method: This study was focused on the use of vibration measurements as one of the main methods of condition monitoring of diesel engines. Today, many methods are being used to diagnose the diesel engine faults that can be shown as follows: Diagnosing the fault by making use of ionic current. That is, identifying the fault by the change of it between the electrodes, when the cylinder is working (Wang and Zhou, 2003). Detect the fault by the waveform of ignition voltage. That is, to diagnose the fault on the based on the difference of ignition voltage waveforms in various working conditions (Chao *et al*., 2008). Diagnose the failure by the engine cylinder pressure. That is, to calculate the indicated mean effective pressure by measuring the pressure in engine cylinders and to compare it with that of the normal condition (Villarino and Bohme, 2004), then the fault can be distinguished from the result. Detecting the fault by the oxygen was contained in the exhaust gas. That is, to measure the oxygen density at the end of the exhaust pipe in the engine. A higher oxygen density than that of the normal working conditions indicates the fault in the engine (Chung *et al*., 2000). Diagnose the fault by the rotation speed of the crankshaft. That is, to establish the linear or non-linear dynamics model of an engine. Then identify the working conditions by the deviation of transient rotation speed of the engine principal shaft (Jiang *et al*., 2007). Fault detection by vibration signal of the cylinder head. That is, to install the sensors on the cylinder head bolts. Compared to the above methods; the vibration signal of the cylinder head is a very easy to measure it has no effect on the working of the engine of the whole progress in measurement. Therefore, this method shows its obvious advantages in the large number of repeatable and non-damaging experiments, which is based on the design of cylinder shape and the configuration of a calibration program. So, in this experiment, vibration signal method was established as the way of recording required data set because of the ease of measurement and the rich contents of the information. Vibration measurement is one of the most common fault diagnosis methods. Vibration signal from the machine surface as the multi-stimulation response, not only contains stimulation information in detail, but also contains the transferring characteristics and relative fault information. Therefore,

it is an effective method to carry out performance of monitoring and fault diagnosis without disassembling the engine (Zhen *et al*., 2004). Several researchers such as Modgil *et al*. (2004), for example, noted that in many cases, there is a direct one-to-one relationship between the cause of the defect and the frequency content and amplitude of the vibration signal. In recent years, these vibration analysis applications have been used to complicated devices that incorporate a large number of moving parts such as reciprocating machines, gear boxes transmissions (Biqing *et al*., 2004) and also in a small number of applications involving internal-combustion engines as done by Mingzan *et al*. (2003). To keep vibrations under control, it is essential to understand the basics and main sources of engine vibrations.

WAVELET TRANSFORMS METHOD AND MULTI-RESOLUTION ANALYSIS

Wavelet transforms method: Wavelet analysis is a method signal process, which decomposes the signal with multi-scale wavelet function and eliminates the strong noise from the original signal. In addition, it is widely used in the processing of complicated signals; therefore, it is significant and practical for the detection of engine fault, i.e., to introduce the wavelet analysis into the analysis of cylinder-head vibration signals. One of the most important issues in intelligent monitoring is that which related to featuring extraction. This research mainly focuses on finding applicable features for diesel engine fault detection and diagnosis. Wavelet Transforms (WT), which is capable of simultaneously processing stationary and non-stationary signals in time and frequency domains, was used for feature extraction (Daubechies, 1992). Despite the amount of previous research on wavelet transform; the selection of the mother wavelet function as a significant topic in signal analysis, has been investigated. WT can mainly be divided into discrete and continuous forms.

Continuous wavelet transforms: Continuous wavelet transform the signal x (t) is defined as Addison (2002):

$$x_{wt}(\tau, s) = \frac{1}{\sqrt{|s|}} \int_{-\infty}^{\infty} x(t) \psi^* \left(\frac{t-\tau}{s} \right) dt. \quad (1)$$

The signal-transformed coefficient X_{wt} (τ, s) is a function of the translation parameter (time parameter τ) i.e., the mother wavelet and the scale parameter s i.e., father wavelet (s>0). The mother wavelet is denoted by ψ (t), the * indicates that the complex conjugate is used in case of a compound wavelet. The signal energy is normalized at every scale by dividing the wavelet coefficient by $1/\sqrt{|s|}$ (Addison, 2002). This ensures that the wavelets have the same energy at every scale or the reason for choosing the factor $1/\sqrt{|s|}$ in Eq. (1) is to keep the energy of the wavelets constant.

Given ψ (t) is the mother wavelet the other wavelets can be calculated as follows:

$$\psi_{s,\tau}(t) = \left(\frac{1}{\sqrt{s}} \right) \psi \left(\frac{t-\tau}{s} \right) dt \quad (2)$$

where, s and τ are the dilation and translation parameters, respectively, $s \in R^+ - \{0\}, \tau \in R$, (Amaris *et al*., 2008).

The Discrete Wavelet Transform (DWT), instead of (CWT), was used in this study (Misiti *et al*., 1996). Calculations were made for a chosen subset of scales and positions. Recently, Daubechies built orthogonal wavelet that was a simple, but it is very skillful, in addition; he has done many studies on wavelet frameworks that allow more freedom regarding the choice of the foundation wavelet functions at less expense of some abundance. Daubechies, along with Mallat, therefore, is entrusted for the improvement of the wavelet from continuous to discrete signal analysis. In the DWT formalism, the scale s and time τ are discretized as follows:

$$s = s_0^m \quad \tau = \mathrm{n}s_0^m \ \mathrm{s}_0 > 0 \text{ And } m \in Z \quad (3)$$

where, m and n are integers. Therefore, the continuous wavelet function ψ (t) becomes discrete wavelets and given by:

$$\psi_{m,n}(t) = s_0^{-m/2} \psi \left(s_0^{-m} t - n\tau_0 \right). \quad (4)$$

The discretization of the scale parameter and time parameter leads to the discrete transform, which defined as:

$$X_{wt}(m, n; \psi) = s_0^{-m/2} \int x(t) \psi^* \left(s_0^{-m} t - n\tau_0 \right) dt. \quad (5)$$

Different from the STFT, the wavelet transform can be used for multi-scale analysis of a signal through dilation and translation, so it can effectively extract time-frequency features of that signal. Therefore, the wavelet transform is more suitable for the analysis of non-stationary signals (Francois and Patrick, 1995). Nowadays, the wavelet obtains great success in machine fault diagnosis for its many distinct advantages, i.e., not only for its ability in the analysis of non stationary signals; but also the wavelet coefficients in the different frequency bands of the DWT can be processed in several ways. By adjusting the wavelet coefficients the reconstructed signal of the synthesis

filter bank can be changed in comparison to the original signal; this gives the DWT some more attractive properties over linear filtering. Compared to the CWT, DWT is simply to compute and its coefficients are easier to interpret since no conversion from scale to frequency has to be made.

This scheme was conducted by computing the so-called approximations and details coefficients. The approximations coefficients are high-scale and low frequency components, while the details ones are low-scale and high frequency components of the signal. The DWT coefficients were computed using the equation:

$$x_{s,\tau} = x_{j,k} = \sum_{n \in Z} x[n] g_{j,k}[n] \quad (6)$$

where,

$$s = 2^j, \tau = k2^j, j \in N, k \in Z$$

The wavelet filter g plays the role of ψ (t).

The decomposition (filtering) process can be iterated, so that one signal can be broken down into many lower-resolution components; this is called the wavelet decomposition tree. For detection of transients, a multi-resolution analysis tree based on wavelets has been applied (Mallat, 1998). Figure 4 showed the tree structure of 5 level multi-resolution decomposition. Every one of the wavelet transforms sub-band was independently reconstructed from each other, so as to get k+1 separated components of the signal x [n]. The MATLAB multires function (Sanchez *et al*., 1996) calculates approximation coefficients to the 2^k scale and detail coefficients signals from the 2^1 to the 2^k scale for a given input signal. It uses the analysis low-pass and high-pass filters to synthesize those filters again to get the original signal. The decomposition can be halted at any scale with the final smoothed output containing the information of all the remaining scales.

Multi-resolution analysis: The discrete wavelet analysis is based on the concept of Multi-Resolution Analysis (MRA) introduced by Mallat (1998). With the (MRA), the signal was decomposed recursively into a sum of details and approximations coefficients at different levels of resolution. From the low-pass filter, a vector of Approximation Coefficients (*CA*1) was found that represents an estimation of original signal with half resolution. From the high-pass filter, a vector of Detail Coefficients (*CD*1) was obtained that contains the details of the signal. The vector (*CA*1) can be further decomposed to form of a new vector of Approximation Coefficients (CA2) and a vector of Detail Coefficients (*CD*2). With the increase of the decomposition level,

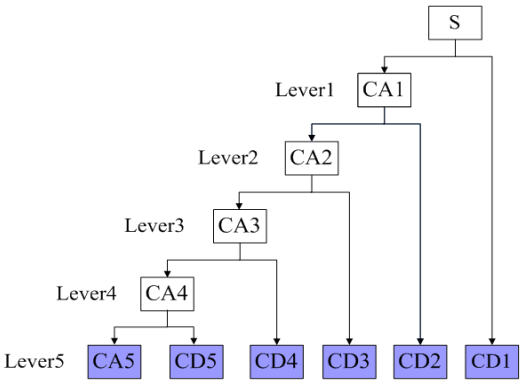

Fig. 4: Decomposition tree of DWT signal S. CD and CA are details and approximations coefficients at levels 1-5

Less information will be included in the approximation coefficients. The lost information between approximation coefficients of too successive decompositions is encoded into the detail coefficients; this process can be iterated to level *N*. In this study; iteration was made to level 5 and db order 5. As a result, a vector of approximation coefficients and a series of vectors of detail coefficients were accomplished that forms the DWT coefficients. For instance, if F_s is the sampling frequency, then the approximation of a level-N of the DWT decomposition corresponds to the frequency band $(0, \frac{F_S}{2^{N+1}})$, whereas the detail covers the frequency range $(\frac{F_S}{2^{N+1}}; \frac{F_S}{2^N})$. The relation of 5-level multi-resolution decomposition at original signal S is noted mathematically as:

$$S = CA5 + CD5 + CD4 + CD3 + CD2 + CD1$$

where, *D*1 to *D*5 denotes the first to five multi-resolved higher frequency signal (details coefficients), while, *A*5 denotes the lowest frequency signal (approximation coefficient). The signal can be conveniently reconstructed by Inversing Discrete Wavelet Transform (IDWT).

As shown in Fig. 5 at each stage of the MRA, the signal was passed through a high-pass filter (scaling filter) denoted as *H* and low-pass filter (wavelet filter) denoted as *G*. The *H* and *G* filters are the decomposition filters. The H_0 and G_0 filters are the reconstruction filters; the process of reconstructing the approximations $CA_i(t)$ and details $CD_i(t)$ was presented in Fig. 6.

The wavelet coefficients thus obtained can then be used for the purposes of signal denoising and compression.

SIGNAL DENOISING

When a signal was collected from the diesel engine head, it was frequently contaminated by noise; the term

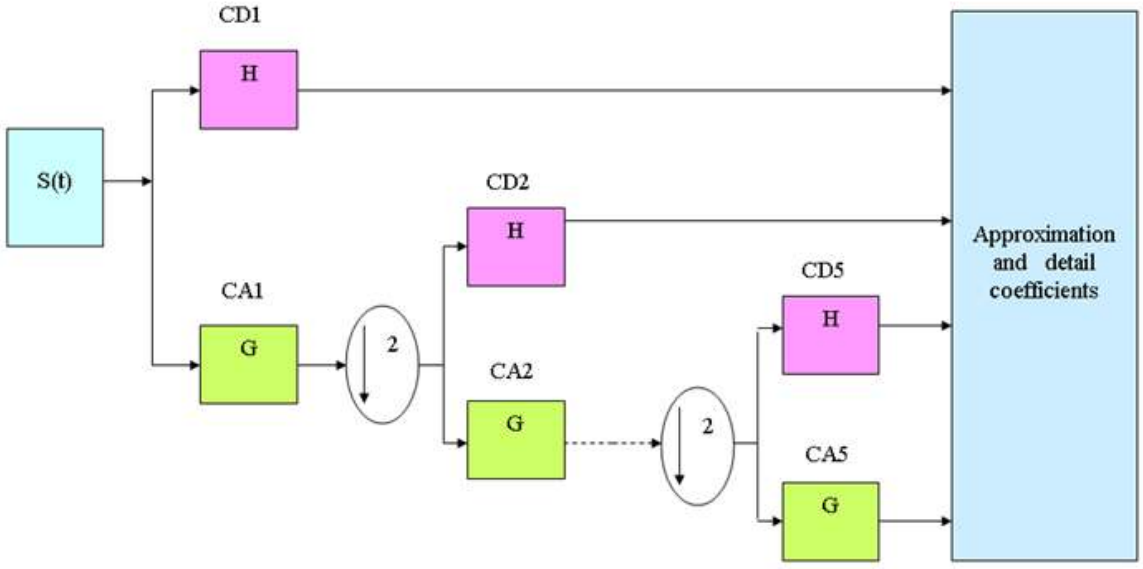

Fig. 5: The decomposition process of approximations (CAi) and details (CDi), at level 5. A symbol ↓2 represent dyadic down sampling

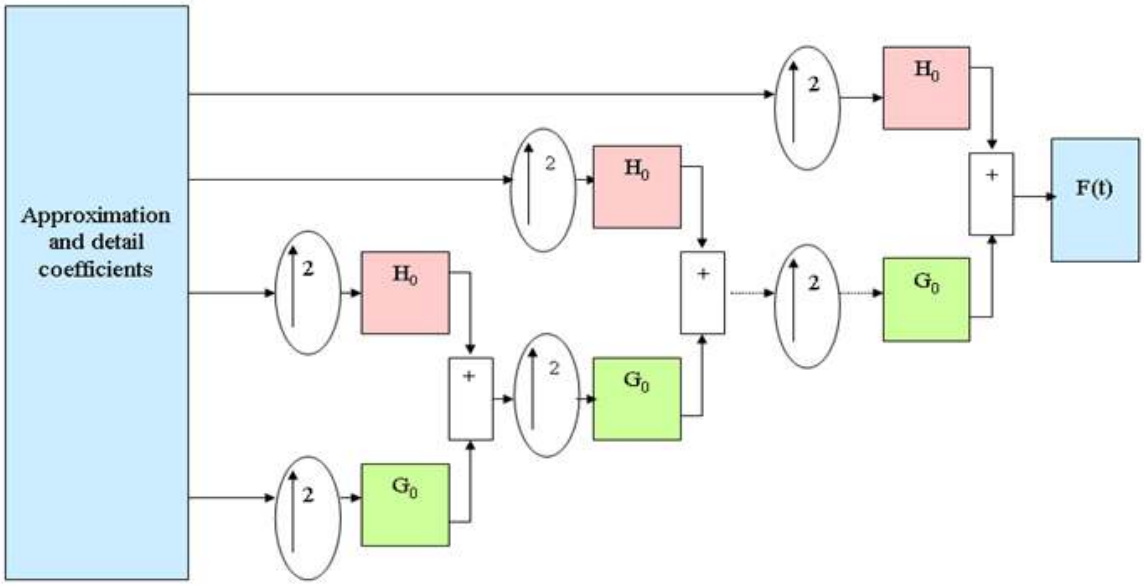

Fig. 6: The reconstruction process of approximations (CAi) and details (CDi), at level 5. A symbol ↑2 represent dyadic up sampling

noise refers to any undesired change that altered the values of the original signal. The simplest model for acquisition of noise by a signal is the additive noise, which has the follows form: contaminated signal = original signal + noise. Reduction of noise as an integral part of signal estimation has been studied for many years in diverse fields such as vibration signals. The principle of denoising method which used DWT is that the wavelet coefficients belonging to the noise at each scale must be removed, while keeping the valuable signal. Finally, the reconstruction of decomposed and de-noised signal can be processed by property of reciprocity.

Method of threshold denoising: From signal denoising, it has been shown that thresholding the wavelet coefficients of a noisy signal allow to restore the smoothness of the original signal. Since the beginning of using wavelet transforms in signal processing, it has been noticed that wavelet threshold was gained considerable interest for removing noise from signals. The method consists of decomposing the

data into an orthogonal wavelet basis, to suppress the wavelet coefficients smaller than given amplitude; and therefore, to transform the data back into the original domain. In this research, the use of discrete wavelet transforms for denoising diesel engine head vibration signals have been investigated. Because of the large bandwidth of the diesel engine head systems, the vibration signal is usually contaminated by noise coming from various sources such as the crank mechanism, pressure pulses from gas, fuel or air flow, valves, gearwheels, an unbalanced turbocharger and so on. Denoising the diesel engine head vibration signals before performing any data analysis is very important in order to enhance the showing of detection of the diesel engine faults and to get correct depth results (Lahouar, 2003).

Energy is mostly concentrated in a small number of wavelet dimensions; the coefficients of these dimensions are relatively large compared to the other dimensions or to noise, which has its energy spread over a large number of coefficients. Hence, by setting smaller coefficients to zero, the noise can nearly optimally be eliminated, while preserving the important information of the original signal (Donoho, 1995).

Types of thresholding: Two standard threshold techniques exist; these are soft threshold (shrink or kill) and hard threshold (keep or kill). These two thresholding methods are used to estimate wavelet coefficients in wavelet threshold de-noising (Merry, 2005). The simplest threshold technique is the hard threshold, where the new values of the details coefficients, $cd^{\wedge}(t)$ were found according to the following equation:

$$cd^{\wedge} = \begin{cases} cd(t) & if\ |cd(t)| > \theta \\ 0 & if\ |cd(t)| \le \theta \end{cases} \quad (7)$$

where,
$cd(t)$ = The details coefficients
θ = The threshold level

In the soft threshold, the new details coefficients were given by the following equation:

$$cd^{\wedge} = \begin{cases} sign(cd(t))(|cd(t)| - \theta) & if\ |cd(t)| > \theta \\ 0 & if\ |cd(t)| \le \theta \end{cases} \quad (8)$$

where, *sign* () is the sign function.
The threshold θ can be estimated as follows:

$$\theta = \sigma\sqrt{2long(N)} \quad (9)$$

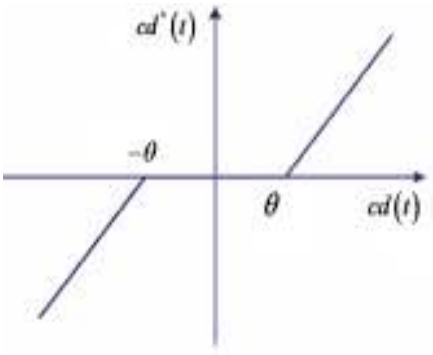

Fig. 7: Hard threshold denoising

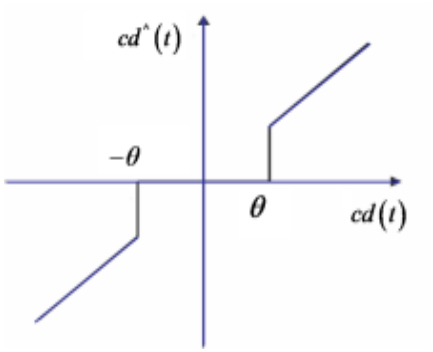

Fig. 8: Soft threshold denoising

where, N is the length of threshold coefficients and σ characterizes the noise level. This method of threshold selection and others were described in Donoho and Johnstone (1995).

In order to get the denoised signal, the new details coefficients, $c\hat{d}$ (t) are used in the signal reconstruction process instead of the original coefficients CD (t). Figure 7 and 8 illustrated the difference between the hard and soft thresholds denoising methods respectively; these methods have been widely used in data processing. The procedure of signal denoising based on DWT consisted of three steps: decomposition, thresholding and reconstruction signal. The denoising procedure is summarized in Fig. 9.

The contrast, Signal to Noise Ratio (SNR) and Root Mean Square Error (RMSE) were used to stimulate the noise cancellation effect. When SNR is greater than RMSE, the signal is closer to the original signal and the noise was reduced or removed.

When the x (n) was chosen for the original signal and $\hat{x}$ (n) for the signal after denoising; then SNR can be defined as follows:

$$SNR = 10\log\left[\frac{\sum_n x^2(n)}{\sum_n \left[x(n) - x^{\wedge}(n)\right]^2}\right] \quad (10)$$

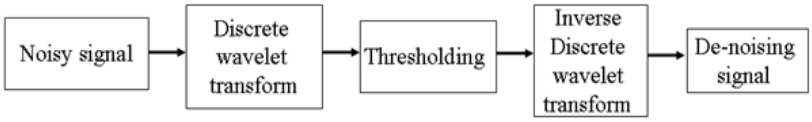

Fig. 9: Discrete wavelet transforms denoising procedure

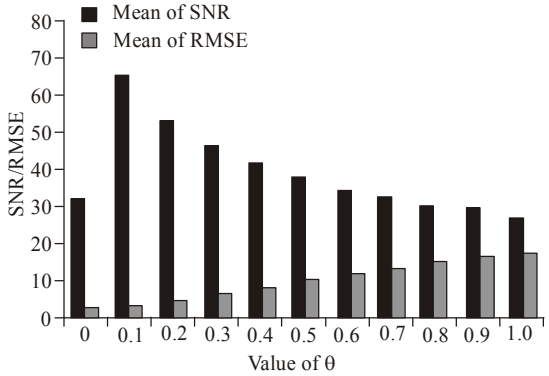

Fig. 10: Comparison of SNR and RMSE under different values of θ

While the RMSE can be defined by the following equation:

$$RMSE = \sqrt{\frac{1}{N}\sum_{n}\left[x(n)-\hat{x}(n)\right]^2} \quad (11)$$

Selection of the optimum threshold level and mother wavelet decomposition for the signal denoising: The selection of the threshold level θ that ranges from 0.0-1.0 plays an significant role in the denoising process, which is manifested by the cancellation of the noise. Therefore, selection of the appropriate value of θ is very important. In order to use a suitable mother wavelet and decomposition level N for denoising signal, several tests on the selected samples (4096 samples) were done. From those tests, it was cleared that the best mother wavelet and level N are sym5 and level 5, respectively. The average of SNR and RMSE were compared. The results were plotted in histograms form Fig. 10. Knowing that the difference between SNR and RMSE is very big, so to compare SNR and RMSE, the RMSE was multiplied by 10 (RMSE×10), as shown in Fig. 10.

From Fig. 10, it is clear that, when θ = 0.1 the average of SNR was 67.0272, which is the biggest value and greater than that of the RMSE. This means that the signal is closest to the original signal and the noise was reduced or removed. Therefore, this was considered as the best hard threshold level to use for denoising process.

Selection of mother wavelet and wavelet decomposition level for signal analysis: There are many different mothers' wavelets that playing an important role in the impact of noise cancellation (Hu and Kw, 2010). The selection of mother wavelet is one of the main factors to maintain the data in the wavelet domain. According to Peretto *et al*. (2005), the effectiveness of the wavelet analysis is largely influenced by the choice of the mother wavelet, decomposition level and the noise cancellation. The choice of the appropriate mother wavelet depends on the nature of the signal and the type of the information to be extracted from the signal. In this study, in order to select the best mother wavelet and decomposition level of the wavelet function; many several tests have been done in many types of wavelet functions such as Daubechies, Symlet, Haar and Coiflet wavelet families. The selected mother wavelet type should be one that has the greatest value of the SNR. The `db5' mother wavelet and wavelet decomposition level 5 have the best performance than others. Accordingly, they were applied in this research studied.

BACK PROPAGATION NEURAL NETWORK

Artificial Neural Network (ANN) is non-linear mapping structures based on the function of the human brain. It is a powerful tool for modeling, especially when the underlying data relationship is unknown. ANN can identify and learn correlated patterns between input data sets and corresponding target values. After training, ANN can be used to predict the outcome of new independent input data. ANN has a great capacity in predictive modeling, i.e., all the characters describing the unknown situation can be presented to the trained ANN and then predicts the results. In recent decades, ANN has been used for a wide variety of applications such as chemical processes, engineering, digital circuitry and control systems. It should be noted that, choosing a suitable ANN architecture is very important for its successful application. A neural network consists of a set of connected cells, i.e., the neurons. The neurons receive impulses from either input cells or other neurons, perform some kinds of transformation of the input and transmit the outcome to other neurons or to output cells. The neural networks are built from layers of connected neurons; one layer receives input from the preceding layer of neurons and passes the output on to the subsequent layer. To date, the most popular ANN architecture is the backward propagation neural network BPNN (Ying *et al*., 2010). Furthermore, neural networks are capable of performing fault classification at hierarchical levels. Based on learning strategies, ANN falls into two categories namely

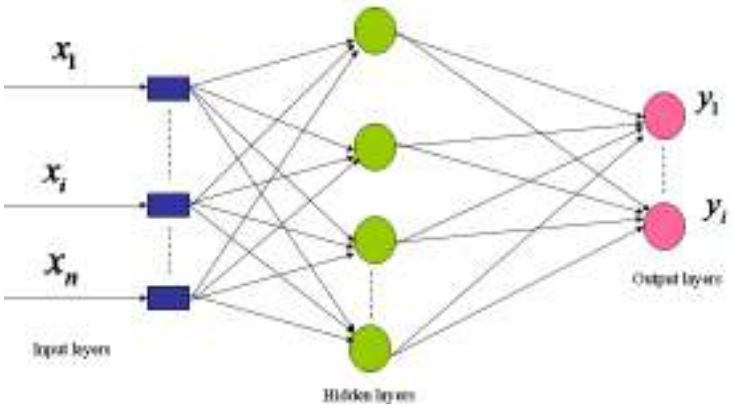

Fig. 11: Model of back-propagation network

supervised and unsupervised. The BPNN is a supervised network and a model of it was shown in Fig. 11. Each input node is connected to a hidden layer node and each of it is connected to an output node in a similar way. This makes the BPNN a fully connected network. The outputs are compared to the desired target values and an error was produced. In addition, the weights are adapted to minimize the error. Finally, the desired target value was known; then this is a supervised learning process.

The input values (input data) are fed to the neurons in the so-called input layer in the left part of Fig. 11. Then these values are processed within the individual neurons of the input layer. After that, the output values of these neurons are forwarded to the neurons in the hidden layer. The arrows indicate the connections from the input nodes to hidden nodes; along which the output values of the input nodes are passed on to the hidden nodes. Either these values obtained as inputs by the hidden nodes, which processed within them and passed on to the output layer or to the next middle layer, i.e., there are more than one hidden layer. Each connection has an associated parameter indicating the strength of it; the so-called weight. By changing the weights in a specific manner, the network can "learn" to map patterns presented at the input layer to targeted values of the output layer. The description of the procedure by which this weight adaptation is performed is called learning or training algorithm. Sometimes, the so-called bias units are also present in the neural network; these are neurons with the property of always producing $a+1$ at the output (Hurvich and Tsai, 1989). The back propagation algorithm is the most commonly used ANN learning technique. For a three-layer network with n input, h number of hidden neurons and m output neurons, the number of neurons in hidden layer would be obtained as follows:

$$h = \sqrt{n*m}+c \tag{12}$$

where,
c : A constant, usually take from 1-20

The hidden node output y_i is calculated as follows:

$$y_i = f\left(\sum_j w_{ij}x_j - \theta_j\right) \tag{13}$$

where,
x_j = The input to the input node
w_{ij} = The input layer to hidden layer connection weight
θ_j = The threshold for the hidden layer nodes

The output node of the output o_i can be found by the following formula:

$$o_i = f\left(\sum_i T_{ij}y_i - \theta_i\right) \tag{14}$$

where,
T_{ij} = The hidden layer to output layer connection weights
θ_i = Threshold for the output layer nodes

The following equation is used to calculate the error control:

$$E = \sum_{k-1}^{p} e_k < \varepsilon \tag{15}$$

$$e_k = \sum_{l-1}^{L}\left|t_1^{(k)} - o_l^{(k)}\right|^2 \tag{16}$$

where,
E = The error for all samples
e_k = The error for one sample
p = The number of samples
o_i = The output nodes
t_l = The desired output of output node

Calculation of error value δ is performed as follows:

$$\delta_1 = (t_1 - O_l) \cdot O_l \cdot (1 - O_l) \quad (17)$$

Weight correction can be obtained as follows:

$$T_{li}(k+1) = T_{li}(k) + \eta \delta_l y_i \quad (18)$$

Threshold correction can be found as follows:

$$\theta_l(k+1) = \theta_l(k) + n\delta_1 \quad (19)$$

Hidden layer node is revised as follows:
Error can be obtained as follows:

$$\delta_i^{'} = y_i(1-y_i)\sum \delta_l T_{li} \quad (20)$$

Weight correction can be calculated as follows:

$$w_{ij}(k+1) = w_{ij}(k) + \eta^{'}\delta_i^{'} x_j \quad (21)$$

Threshold correction can be obtained as follow:

$$\theta_i(k+1) = \theta_i(k) + \eta^{'}\delta_i^{'} \quad (22)$$

SUPPORT VECTOR MACHINE AND SIGNAL PATTERN RECOGNITION

Support Vector Machine (SVM) is a useful technique for data classification. According to Vapnik *et al*. (1996), there are three main problems in machine learning, which are: classification, regression and density estimation. In all the cases, the goal is to suppose a function from a sample data. In the supervised learning model, the training data consists of pairs of input/output points (x_i, y_i), $1 \le i \le n$, with x_i belonging to some space X and $y_i \in R$ (regression) or $y_i \in \{-1, 1\}$ (binary classification). In machine condition monitoring and fault diagnosis problem, SVM is employed for recognizing special patterns from acquired signal and then these patterns are classified according to the fault occurrence in the machine. After signal acquisition, a feature representation method can be performed to define the features, e.g., statistical feature of signal for classification purposes. These features can be considered as patterns that should be recognized using SVM. Usually, huge features will be obtained in feature representation. Unfortunately, not all features are meaningful and contain high information about machine condition; some of them are useless and irrelative features. These features should be removed to increase the accuracy of classifier. Therefore, feature extraction and selection are needed to produce good features for classification routines (Barzilay and Brailovsky, 1999).

Construction of SVM algorithm: Support vector machine is a useful classification method Boser *et al*. (1992). Given the data input x_i (i = 1, 2, 3 … L), L is the number of samples; the samples are assumed to have two classes namely positive class and negative one. Each of these classes is associated with labels be y_i = 1 for positive class and y_i = - 1 for negative class. In the case of linear data, it is possible to determine the hyper-plane $f(x) = 0$ that separates the given data or linearly separate the training set of $\{x_i, y_i\}, x_i \in R^n, y_i = \{+1, -1\} (i = 1, 2, ..., l)$; there are real even number sequences (w, b) that satisfy the conditions:

$$\begin{cases} w.x_i + b \ge 1 & (y_i = +1) \\ w.x_i + b \le -1 & (y_i = -1) \end{cases} \quad (23)$$

Classification function from the above conditions is as follows:

$$f(x) = sign(w.x_i + b) \quad (24)$$

The separating hyper-plane that creates the maximum distance between the plane and the nearest data, i.e., the maximum margin, is called the optimal separating hyper-plane. Taking into account the noise with slack variables g_i and the error penalty c, the optimum hyper-plane that separating the data can be obtained as a solution to the following optimization problem:

$$\text{Minimize } D_{\min} = \frac{1}{2}\|w\|^2,\ D_{\min} = \frac{1}{2}\|w\|^2 + C\sum_{i=1}^{l} g_i \quad (25)$$

$$\text{Subjected to } y_i(w.x_i + b) \ge 1 \quad (i = 1, 2, ..l)$$

The calculation can be simplified by converting the problem with Kuhn-Tucker condition into the equivalent Lagrangian dual problem, which will be as follows:

$$L(w, b, a) = \frac{1}{2}\|w\|^2 - \sum_{i=1}^{l} a_i \left[y_i (w.x_i + b) - 1 \right] \quad (26)$$

In which the Lagrange multiplier $a_i \ge 0$.

The task is to minimize Eq. (26) with respect to w and b, while requiring the derivatives of L to a to

vanish. At an optimal point, the following saddle-point equations can be obtained:

$$\frac{\partial L}{\partial w} = 0, \quad \frac{\partial L}{\partial b} = 0, \tag{27}$$

This was replaced into the following form:

$$w = \sum_{i=1}^{l} a_i y_i x_i, \quad \sum_{i=1}^{l} a_i y_i = 0 \left(a_i \geq o\right) \tag{28}$$

From Eq. (28), w was found to be contained in the subspace spanned by the x_i. By substituting Eq. (28) into (26), the dual quadratic optimization problem was obtained as follows:

$$\text{Maximize } L(a) = \sum_{i=1}^{l} a_i - \frac{1}{2} \sum_{ij=0}^{l} a_i a_j y_i y_j x_i . x_j \tag{29}$$

$$\text{Subjected to } a_i \geq o, \quad i = 1,...,l, \quad \sum_{i=1}^{l} a_i y_i = 0. \tag{30}$$

Thus, by solving the dual optimization problem the coefficient a_i, can be obtained, which was required to express the w to solve Eq. (25). This leads to the following non-linear decision function:

$$f(x) = sign\left(\sum_{ij=1}^{l} a_i y_i x_i . x_j + b \right) \tag{31}$$

SVM can also be used in non-linear classification tasks with application of kernel functions. The data to be classified is mapped onto a high-dimensional feature space, where the linear-classification is possible. Using the non-linear vector function $\varphi(x) = (\phi_1(x),\ldots, \phi_l(x))$ to map the n-dimensional input vector x onto l dimensional feature space, the linear decision function in a dual form was given by:

$$f(x) = sign\left(\sum_{ij=1}^{l} a_i y_i \left(\phi(x_i) . \phi(x_j) \right) + b \right) \tag{32}$$

Working in the high-dimensional feature space enables the expression of complex functions, but it also generates a problem. Computational problem occurred due to the large vectors and the over-fitting exists due to the high-dimensionality. The latter problem can be solved by using the kernel function $K(x_i, x_j)$. Kernel is a function that returns a dot product of the feature space mappings of the original data points and stated as:

$$K(x_i, x_j) = \left(\phi(x_i) . \phi(x_j) \right)$$

When applying a kernel function, the learning in the feature space does not require explicit evaluation of ϕ and the decision function will be as follows:

$$f(x) = sign\left(\sum_{ij=1}^{l} a_i y_i K\left(x_i, y_j\right) + b \right) \tag{33}$$

Any function that satisfies Mercer's theorem Chebil *et al*. (2009) can be used as a kernel function to compute a dot product in the feature space. There are different kernel functions used in SVM, such as linear, polynomial and Gaussian Radial Basis Function (RBF). The selection of the appropriate kernel function is a very important, since the kernel defines the feature space in which the training set examples will be classified. The definition of legitimate kernel function is given by Mercer's theorem. In this study, linear, polynomial and RBF were evaluated and formulated as follows:

Linear kernel:

$$K(x_i, x_j) = x_i \cdot x_j \tag{34}$$

Polynomial kernel:

$$K(x_i, x_j) = (x_i \cdot x_j + 1)^3 \tag{35}$$

RBF kernel:

$$K(x_i, x_j) = \exp\left\{ -\left| x_i - x_j \right|^2 \Big/ 2\delta^2 \right\} \tag{36}$$

where, δ is kernel parameter.

RESULTS AND DISCUSSION

Wavelet analysis on cylinder head vibration signal: Original cylinder head vibration signal not only included low-frequency signal, but also included complicated high-frequency signal. Consequently, it is difficult to discriminate directly between healthy and faulty behaviors from the original signals, especially in high-speed segment. Thereby, the fault can be clearly distinguished after decomposing the signals. When a defect occurs, the engine vibration accelerates and the signal frequencies and amplitudes will be changed. Therefore, the output signal energy distribution will change. For example, some frequency-domain signals are suppressed, while others are enhanced, which result in a corresponding decrease or increase in an energy. In this study, the DWT decomposition was applied to the vibration data for normal and abnormal condition, using mother wavelet *db*5 and decomposition level 5. The

Table 2: Frequency sub-bands for the six levels of DWT decomposition

Frequency bands	1	2	3	4	5	6
Frequency range (Hz)	0-136	136-264	264-519	519-1030	1030-2052	2052-4096
	CA5	CD5	CD4	CD3	CD2	CD1

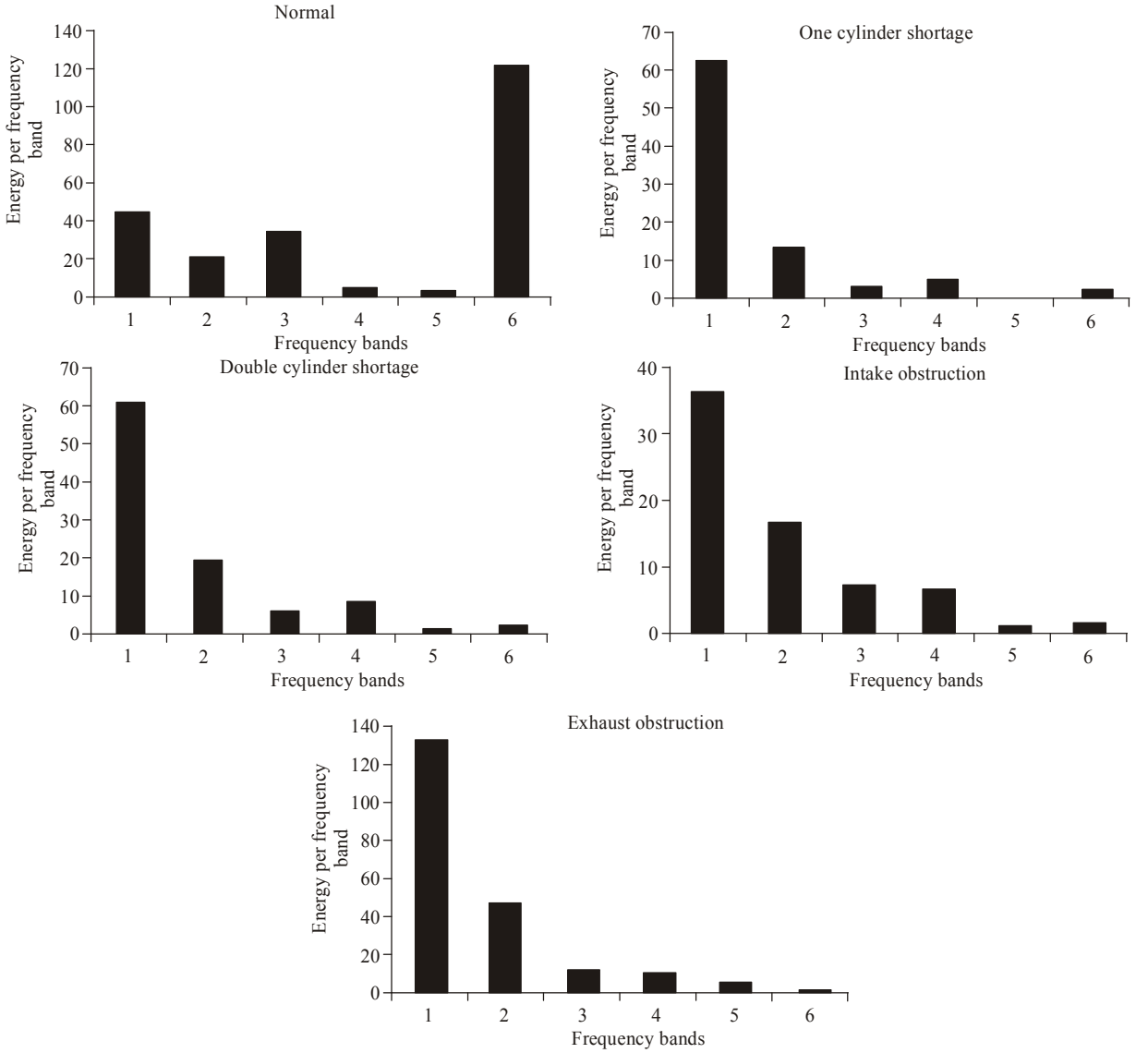

Fig. 12: Average energy contained in the frequency sub-bands of 1, 2, 3, 4, 5 and 6 for vibration data captured on a surface of the cylinder head of the 295 diesel engine

original Signal (*S*) was decomposed into six components: an approximation coefficient *CA*5 and five details coefficients from *CD*1 to *CD*5. The frequency sub-bands corresponding to each component of the signal were shown in Table 2.

Characteristics of the signal energy extraction and fault detection: The analysis of the energy characteristics of the signal can be used for the diesel engine fault detection. Therefore, the energy was extracted from each frequency sub-band of normal and abnormal conditions as a feature of engine fault diagnosis. Any method developed for this purpose should be highly accurate. There is an approach, which based on the fact that, faults are translated into low and high frequencies phenomena in the vibration signal. Consequently, the failure behavior can be detected by analyzing the energy contained in those frequencies. When this approach was applied to the sub-band frequency, the energy in the sixth band was always higher if the condition is normal, while it was larger in the first band if the condition is abnormal. This result agreed with (Boser *et al*., 1992), who applied discrete wavelet decomposition for the detection and diagnosis

of faults in rolling element bearings. By doing so normal and abnormal conditions, behavior could be efficiently distinguished by comparing the energy accumulation of each sub-band. Figure 12 showed the results of the energy contained in the frequency sub-bands of 1, 2, 3, 4, 5 and 6 for vibration data of healthy and faulty conditions.

Design of the Back-Propagation (BP) network: The BP model used in this study was included in MATLAB Neural Network Toolbox. In this application, the number of inputs X_i is associated with the number of details coefficients extracted from discrete wavelet analyzed. The number of hidden layers and the number of neurons in the hidden layer are generally application dependent. For this study, one hidden layer was used for the whole test, while the number of neurons in this layer was 19; that is to observe the change in classification accuracy. There were five outputs y_i, which were associated with the number of diesel engine fault conditions. The output from the network is binary i.e., each output node is either 0 or 1. On the creation of the BP network function "newff" was used; the input layer and middle layer of the transfer function was "tansig", the middle layer and output layer transfer function was "purelin" while, training function was "trainlm". Weights and threshold value of the BP learning algorithm that used the default gradient and descent momentum learning function was "learngdm". The mean square error for the default performance function is the "mse" and the network training error of 0.001 was selected. Five working conditions namely exhaust obstruction, intake obstruction, normal, single cylinder shortage and double cylinders shortage that corresponded to the desired output of 10000, 01000, 00100, 00010 and 00001, respectively were selected. For example, when the output was 10000 recognition results were of the exhaust obstruction.

Features extraction using BPNN and SVM: Figure 13 illustrated a comparison of the diagnostic accuracies rates extracted as percentages, using SVM and BPNN on the five diesel engine fault conditions. They were applied to the signal captured from the test diesel engine at two speeds, two loads and five fault conditions. The experimental results showed that, diagnosis accuracy of BPNN in the fault detected has higher rates than that of SVM for all cases. These results agreed with Wu *et al*. (2008), who applied artificial neural network and SVM to diagnose the learning disabilities' problem for students. His results showed that neural network performs better than SVM. In addition from Fig. 13, it can also be seen that the normal condition has the highest accuracies rate for all conditions, i.e., almost about 100% when BPNN was applied, but it has got different percentages when SVM was applied. Therefore, it can be observed that BPNN is most consistent in all the conditions than SVM. Finally, according to the above results, it can be concluded that the BPNN is the excellent method than SVM in fault diagnosis for a diesel engine in the cases studied.

Design of the support vector machine training: Support vector machine on different training fault classifications has been used in this study. Just as BPNN was modeled, SVM Toolbox was also used in MATLAB software. In this application, the number of inputs X_i was associated with the number of details coefficients that were extracted from discrete wavelet analysis. The number of outputs y_i was associated with above-mentioned five diesel engine fault conditions.

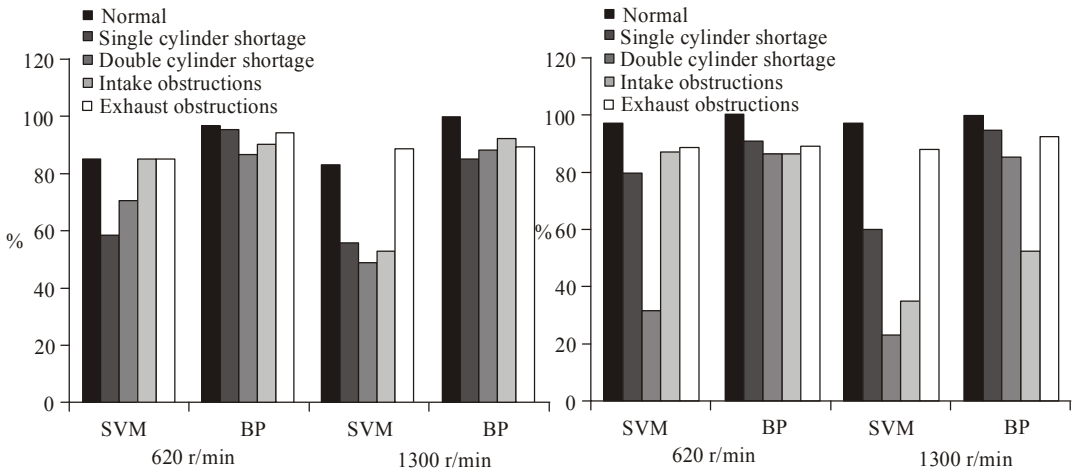

Fig. 13: Classification accuracy rates as (percentages) extracted from SVM and BPNN on the data, at two speeds, two loads and under five fault conditions, (a) load 15 N·m, (b) load 45 N·m

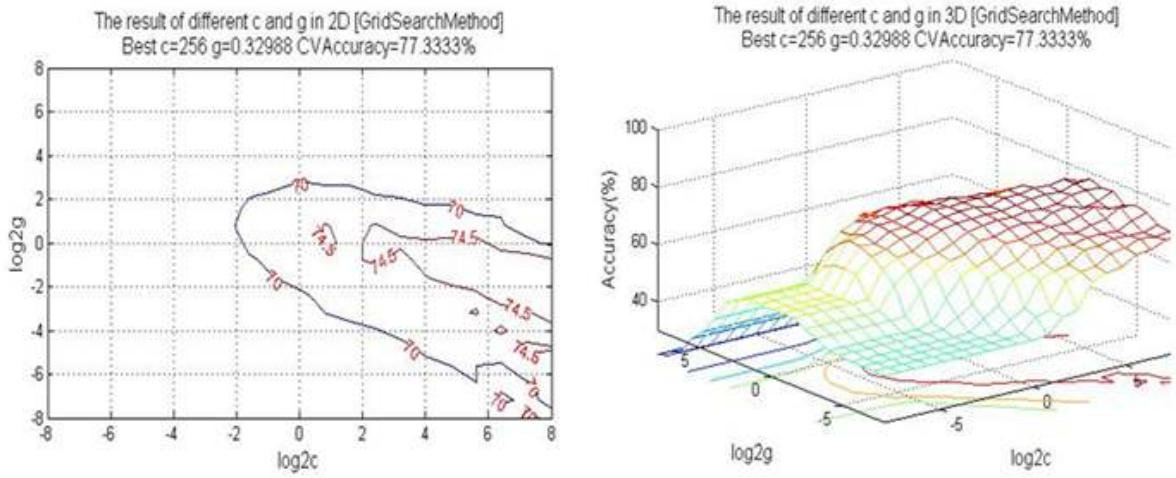

(a) (b)

Fig. 14: Optimization of c and g of engine speeds at 620 rpm

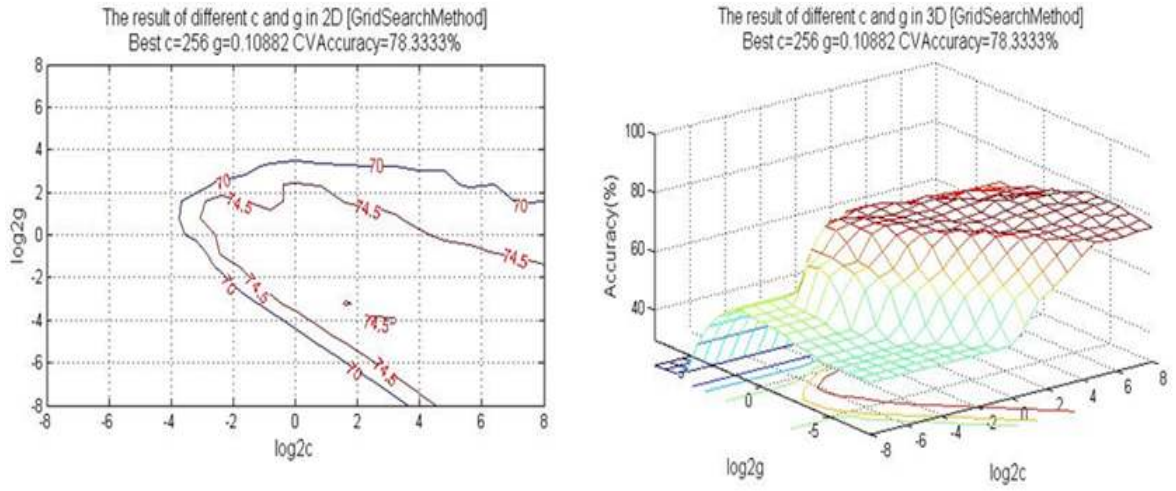

(a) (b)

Fig. 15: Optimization of c and g of engine speed at 1300 rpm

There are two parameters in the RBF kernel. Parameter *c* is the error penalty function and the parameter *g* is the kernel functions. In the function "svmtrain", *c* and *g* were usually given empirically or by any calculation to obtain the Cross-Validation (CV). CV is a standard technique for adjusting hyper-parameters of predictive models. The goal was to identify good *c* and *g*; therefore, the classifier can accurately predict unknown data i.e., testing data. So, usually the function "svmtrainforclass" for cross-validation was used to determine the values of c and g, it is noted that, it may not be useful to achieve high training accuracy i.e., a classifier that correctly predicts training data whose class labels are indeed known. The prediction accuracy obtained from the unknown set more precisely reflects the performance on classifying an independent data set. The cross-validation procedure can prevent the over-fitting problem. The current experiment applied the cross-validation data set for the two speeds, two loads and five-engine fault conditions. Figure 14 and 15 below, illustrated cross-validation test results by developing SVM and radial basis function RBF kernel, in order to optimize parameters c and g, in 2D and 3D at two different speeds.

From Fig. 14 and 15, it can be summarized that the cross-validation test accuracy rates were shown as follows:

- When the speed was 620 rpm, best C = 256, g = 0.32988 with cross-validation rate = 77.33%.
- When the speed was 1300 rpm, best C = 256, g = 0.10882 with cross-validation rate = 78.33%.

CONCLUSION

In this experiment, the attention was focused on the investigation of the vibration signal of the 295 diesel engine. Diesel engine fault diagnosis depends on the feature extraction of the signals. The fault diagnosis system was constructed and designed for inspecting the status and fault diagnosis of the diesel engine based on the discrete wavelet analysis and LabVIEW software. The cylinder-head vibration signals were captured through a piezoelectric acceleration sensor, while the engine was running at two speeds of 620 and 1300 rpm and two loads 15 and 45 N·m. Data was gathered from five different conditions such as single cylinder shortage, double cylinders shortage, intake manifold obstruction, exhaust manifold obstruction and normal condition. The signal captured was analyzed by developing DWT technique. Hard threshold (db5) mother wavelet and decomposition level 5 were used. The results showed that, the energy extracted from discrete wavelet analysis techniques could be successfully used in condition monitoring and fault diagnosis of diesel engine faults. In addition, two techniques, BPNN and SVM were applied on signal capturing to determine classification accuracy rate. The results showed that, BPNN was effectiveness in fault diagnosis for internal-combustion engine with various fault conditions than SVM. Further research on the diesel engine to choose an appropriate mother-wavelet and decomposition-level can increase the accuracy rate of faults diagnosis.

REFERENCES

Addison, P.S., 2002. The Illustrated Wavelet Transform Handbook. IOP Publishing Ltd., ISBN: 0-7503-0692-0.

Amaris, A.H., C. Alonso, M.D. Florez, T.J.P. Lobos, J. Rezmer and Z. Waclawek, 2008. Application of advanced signal processing methods for accurate detection of voltage dips. Proceeding of 13th International Conference on Harmonics and Quality of Power, pp: 1-6.

Barzilay, O. and V.L. Brailovsky, 1999. On domain knowledge and feature selection using a support vector machine. Pattern Recog. Lett., 20(5): 475-484.

Biqing, W., A. Saxena, T.S. Khawaja and R. Patrick, 2004. An approach to fault diagnosis of helicopter planetary gears. Proceeding of IEEE AUTOTESTCON, pp: 475-481.

Boser, B., I. Guyon and V.N. Vapnik, 1992. A training algorithm for optimal margin classifiers. Proceedings of the 5th Annual Workshop on Computational Learning Theory, New York.

Carlucci, A.P., F. Chiara and D. Laforgia, 2006. Analysis of the relation between injection parameter variation and block vibration of an internal combustion diesel engine. J. Sound Vib., 295: 141-164.

Chandroth, G.O. and W.J. Staszewski, 1999. Fault detection in internal combustion engines using wavelet analysis. Proceedings Comadem 99. Sunderland, UK, 3: 8.

Chao, H., J. Xu and C. Ji, 2008. Experimental study on the knock control of HCCI engine by methanol and ethanol additives at high load. T. Chinese Soc. Agric. Mach., 3: 23-27.

Chebil, J., G. Noel, M. Mesbah and M. Deriche, 2009. Wavelet decomposition for the detection and diagnosis of faults in rolling element bearings. Jordan J. Mech. Ind. Eng., 3(4): 260-267.

Chung, Y., H. Kim and S. Choi, 2000. Flow characteristics of misfired gas in the exhaust manifold of a spark ignition engine. J. Autom. Eng., 4: 373-381.

Daubechies, I., 1992. Ten lectures on wavelets. Proceeding of CBMS-NSF Regional Conference Series in Applied Mathematics. Society for Industrial and Applied Mathematics (SIAM). Philadelphia, PA, Vol. 61.

Donoho, D., 1995. Denoising by soft thresholding. IEEE T. Inform. Theory, 4l: 6l3-627.

Donoho, D. and I. Johnstone, 1995. Adapting to unknown smoothness via wavelet shrinkage. J. Am. Stat. Assoc., 90: l200-l224.

Francois, A. and F. Patrick, 1995. Improving the readability of time frequency and time scale representations by the reassignment method. IEEE T. Signal. Process., 43: 1068-1089.

Ftoutou, E., M. Chouchane and N. Besbès, 2011. Internal combustion engine valve clearance fault classification using multivariate analysis of variance and discriminate analysis. T. I. Meas. Control, DOI: 10.1177/ 0142331211408492.

Girdhar, P., C. Scheffer and S. Mackay, 2004. Practical machinery vibration analysis and predictive maintenance. Newness, Elsevier, Oxford.

Hu, J.W. and C. Kw, 2010. Wavelet analysis of vibration signal denoising. J. Mech. Eng. Autom., 1: 128-130.

Hurvich, C.M. and C. Tsai, 1989. Regression and time series model selection in small samples, Biometrika, 76: 297-307.

Jiang, A., X. Li, W. Wang, X. Huang, Z. Zhang and H. Hua, 2007. Misfire failure diagnosis of engine based on wavelet analysis. T. Chinese Soc. Agric. Eng., 4: 153-157.

Lahouar, S., 2003. Development of data analysis algorithms for interpretation of ground-penetrating radar data. Ph.D. Thesis, Department of Elect. Eng. Virginia Tech. Blacksburg, VA.

Liu, Y., R. Du and Y. Shu-Zi, 1999. Internal combustion engine cylinder head vibration acceleration signal of the features and diagnostic applications. Huazhong Univ., Technol., 1: 11-15.

Mallat, S.G., 1998. A theory of multiresolution signals decomposition: The wavelet representation. IEEE T. Pattern Anal., 11: 647-693.

Merry, R.J.E., 2005. Wavelet Theory and Applications, a literature study. Eindhoven University of Technology, Control Systems Technology Group. Eindhoven, DCT 2005.53.

Mingzan, W., J. Qie, Q. Gu and H. Shao, 2003. Wavelet package-neural network based on rough set diesel engine vibration signal identification model. Proceedings of the International Conference on Neural Networks and Signal Processing, pp: 185-190.

Misiti, M., Y. Misity, G. Oppenheim and J.M. Poggi, 1996. Wavelet Toolbox User's Guide. MathWorks.

Modgil, G., R.F. Orsagh and M.J. Roemer, 2004. Advanced vibration diagnostics for engine test cells. Proceedings of IEEE Aerospace Conference, pp: 3361-3371.

Parlak, A., H. Yasar, C. Hasimoglu and A. Kolip, 2005. The effects of injection timing on NOx emissions of a low heat rejection indirect diesel injection engine. Appl. Therm. Eng., 25: 3042-3052.

Peretto, L., R. Sasdelli and R. Tinarelli, 2005. On uncertainty in wavelet based signal analysis. IEEE T. Instrum. Meas., 54(4): 1593-1599.

Sanchez, S.G., N.G. Prelcic and S.J.G. Galan, 1996. Uvi Wave-wavelet Toolbox for Matlab, Ver 3.0, University of Vigo, [Online]. Retrieved form: http://www.tsc.uvigo.es/~wavelets/uvi_wave.html, Apr.

Vapnik, V., S. Golowich and A. Smola, 1996. Support vector method for function approximation, regression estimation and signal processing. Adv. Neur. In., 9: 281-287.

Villarino, R. and J. Bohme, 2004. Pressure reconstruction and misfire detection from multichannel structure-borne sound. Proceeding of IEEE International Conference on Acoustics, Speech and Signal Processing (ICASSP'04), pp: 141-144.

Wang, Y. and L. Zhou, 2003. Investigation of the detection of knock and misfire of a spark ignition engine with the ionic current method. P. I. Mech. Eng. D-J. Aut., 217(7): 617-621.

Wang, C., Z. Zhong and Y. Zhang, 2008. Fault diagnosis for diesel valve trains based on time-frequency images. Mech. Syst. Signal Pr., 22: 1981-1983.

Wu, T.K., S.C. Huang and Y.R. Meng, 2008. Evaluation of ANN and SVM classifiers as predictors to the diagnosis of student with learning disability. Expert Syst. Appl., 34(3): 1846-1856.

Ying, D., H. Yigang and S. Yichuang, 2010. Fault diagnosis of analog circuits with tolerances using artificial neural networks. Proceeding of IEEE Asia-Pacific Conference on Circuits and Systems, (APCCAS), pp: 292-295.

Zhen, W., L. Ji, D. Zijia and S. Yanhui, 2004. Non-stationary Fault Diagnosis based on Local-wave Neural Network. In: Yin, F., J. Wang and C. Guo (Eds.), ISNN 2004. LNCS 3174, Springer-Verlag, Berlin, Heidelberg, pp: 549-554.